Chemistry & Biology
Article

Quartromicin Biosynthesis: Two Alternative Polyketide Chains Produced by One Polyketide Synthase Assembly Line

Hai-Yan He,[1,2] Hai-Xue Pan,[1,2] Long-Fei Wu,[1] Bei-Bei Zhang,[1] Han-Bo Chai,[1] Wen Liu,[1] and Gong-Li Tang[1,*]
[1]State Key Laboratory of Bio-organic and Natural Products Chemistry, Shanghai Institute of Organic Chemistry, Chinese Academy of Sciences, 345 Lingling Road, Shanghai 200032, China
[2]These authors contributed equally to this work
*Correspondence: gltang@sioc.ac.cn
http://dx.doi.org/10.1016/j.chembiol.2012.07.024

SUMMARY

The antiviral compounds quartromicins represent unique members of a family of spirotetronate natural products. In this study, a biosynthetic gene cluster of quartromicins was identified by degenerate primer PCR amplification of specific genes involved in the biosynthesis of the tetronate moiety. The biochemical results confirmed that 1,3-bisphosphoglycerate was incorporated into the tetronate ring, and the intermediates of this ring were also reconstructed in vitro. The data also suggested a module skipping strategy for the production of two alternative polyketide chains by the same polyketide synthase assembly line. These findings set the stage for further investigations of the stereodivergent intermolecular cyclization mechanism, and highlight how nature has constructed this type of C2 symmetric molecule through intermolecular dimerization.

INTRODUCTION

Spirotetronate antibiotics are a growing family of natural products with a wide range of biological activities, as exemplified by the antitumor agents tetrocarcin A (TCA; Tomita et al., 1980) and kijanimicin (Waitz et al., 1981; Figure 1A), the antiviral drug MM46115 (Ashton et al., 1990), the antibacterial compounds chlorothricin (CHL; Kawashima et al., 1992) and abyssomicin (ABY; Riedlinger et al., 2004; Figure 1A), and the cholecystokinin B inhibitor tetronothiodin (Ohtsuka et al., 1993). Quartromicins (QMNs; Figure 1B) are an unusual group of spirotetronate natural products isolated from *Amycolatopsis orientalis* Q427-8 that include six components: A_1, A_2, A_3, D_1, D_2, and D_3 (Kusumi et al., 1991; Tsunakawa et al., 1992; Roush and Barda, 2002). This group of compounds exhibits significant antiviral activity against herpes simplex virus type 1, influenza virus type A, and HIV (Tsunakawa et al., 1992; Tanabe-Tochikura et al., 1992). Until 2002, the stereochemical configuration of QMNs was only partly assigned by nuclear magnetic resonance (NMR) analysis (Roush and Barda, 2002). In addition to the remarkable spirotetronate units of this family of products, QMNs possess several unique structural elements. First, the novel 32-member carbocyclic architecture consists of four spirotetronic acid units that are connected by enone linkers in a head-to-tail fashion, resulting in one of only a few macrocyclic compounds whose carbon framework is composed of only C-C linkages. Second, QMN A_3 and D_3 are C2 symmetric, resulting from a junction between diastereoisomeric (*endo*- and *exo*-) spirotetronate subunits. Third, the four contiguous quaternary carbon stereocenters in the spirotetronate fragments (C4/C12 and C4′/C12′ in the *exo* fragments, and C22/C30 and C22′/C30′ in the *endo* fragments) also distinguish them from other spirotetronate antibiotics.

The structural novelty of this family combined with its impressive biological activity has spurred considerable interest in the biosynthesis of spirotetronate antibiotics. The gene clusters of CHL (Jia et al., 2006), kijanimicin (Zhang et al., 2007), TCA (Fang et al., 2008), and ABY (Gottardi et al., 2011) have all been cloned and characterized. Based on a series of in vivo and in vitro experiments, including biosynthetic studies of the tetronate antibiotics tetronomycin (TMN; Figure 1A; Demydchuk et al., 2008; Sun et al., 2008) and RK-682 (Sun et al., 2010), a reasonable biosynthetic route for tetronate moiety has been deduced. In these compounds, a polyketide unit and a glycerol-derived, three-carbon unit (glyceryl-*S*-ACP) are usually used to form the tetronate moiety. It has shown that the polyketide unit is synthesized by a module type I polyketide synthase (PKS), and glyceryl-*S*-ACP is synthesized by an FkbH-like glyceryl-*S*-ACP synthase (ChlD1, KijC, Tmn16, TcaD1, and RkE), which catalyzes D-1,3-bisphosphophoglycerate (1,3-BPG) to dephosphorize and transfer to a discrete acyl carrier protein (ACP; ChlD2, KijD, Tmn7a, TcaD2, and RkF). In RK-682 biosynthesis, a FabH-like 3-oxoacyl-ACP synthase III (RkD) catalyzes both C-C and C-O bond formation to generate a tetronate moiety from glyceryl-S-ACP and the ACP-bound nascent polyketide chain (Sun et al., 2010). However, whether a similar process is used to construct the tetronate moiety in other cases is unclear. Given the fact that symmetric skeletons and spirotetronate subunits with reverse chirality make QMN distinct from other previously studied systems, unique mechanisms should be included in its biosynthetic process. In this work, we identified the QMN gene cluster by using the degenerate primers of the tetronate locus. We then reconstructed the tetronate intermediate in vitro and biochemically characterized a PKS module skipping strategy that is responsible for producing two alternative polyketide chains.

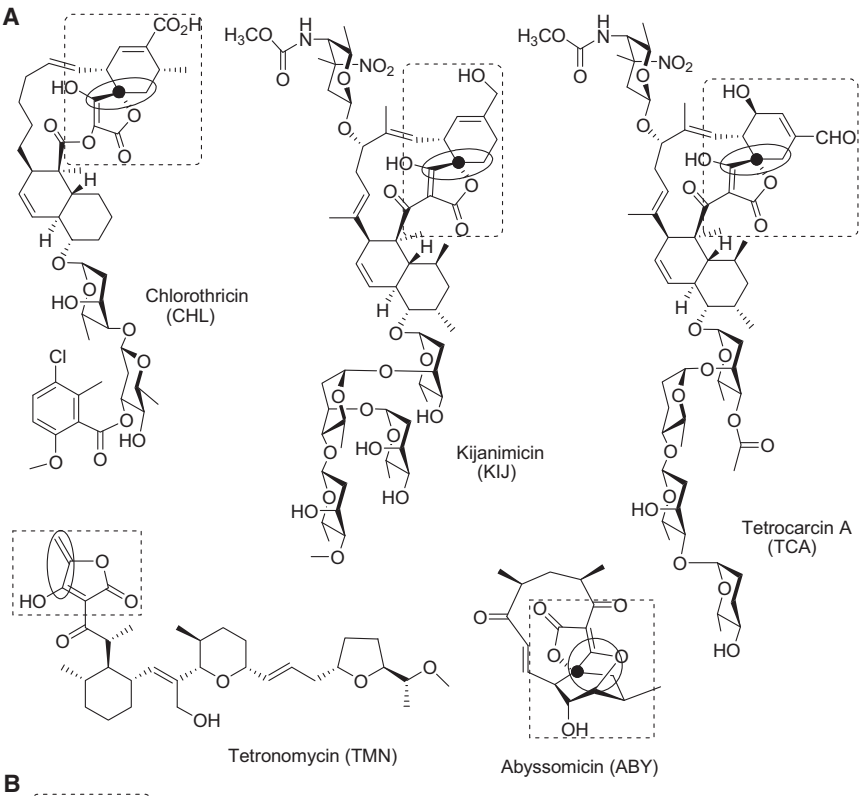

Quartromicin (**QMN**)

	R_1	R_2	R_3
QMN A_1	α-D-Galactopyranosyl	CHO	CHO
QMN A_2	α-D-Galactopyranosyl	CHO	CH_2OH
QMN A_3	α-D-Galactopyranosyl	CH_2OH	CH_2OH
QMN D_1	H	CHO	CHO
QMN D_2	H	CHO	CH_2OH
QMN D_3	H	CH_2OH	CH_2OH

$M^{\oplus}$ = Na^+, K^+, Ca^{2+}

Figure 1. Structures of QMN and Related Natural Products

(A) The tetronate moiety is boxed and the three-carbon unit derived from 1,3-BPG is circled.

(B) The *exo*-spiro center is marked with a black dot and the *endo*-spiro center is marked with a gray dot.

RESULTS

Cloning and Sequencing of the QMN Biosynthetic Gene Cluster

FkbH-like glyceryl-S-ACP synthase is necessary for biosynthesis of the tetronate moiety of spirotetronate antibiotics. Because a homologous enzyme was predicted to mediate the biosynthesis of QMNs, we designed degenerate primers (Table S2 available online) according to the ChlD1 homolog gene encoding FkbH-like glyceryl-S-ACP synthase. Using these primers and the genomic DNA from *A. orientalis* Q427-8 as a template, we acquired a DNA fragment (P1, Figure 2A). We then screened the *A. orientalis* Q427-8 genomic library using the P1 product as a probe, which resulted in several overlapping fosmids spanning a 50 kb DNA region. To ensure full coverage of the entire QMN gene cluster, we conducted chromosome walking from the left end of fosmid pTG4001 by using the PCR product P2 as a probe (Figure 2A). Further chromosome walking using a similar strategy led to a 90 kb contiguous DNA region on the chromosome, which was mapped in two overlapping fosmids (pTG4001 and pTG4002; Figure 2A).

DNA sequencing of the two fosmids yielded an 88,324 base pair (bp) contiguous DNA sequence with 71.4% guanine-cytosine content, which is characteristic of *Amycolatopsis* DNA (Zhao et al., 2010). A bioinformatic analysis of the region revealed 47 open reading frames (ORFs), 28 of which (from *qmnB* to *qmnRg5*; Figure 2A; Table 1) were proposed to constitute the QMN gene cluster according to functional assignment of their deduced products. Genes beyond this region encode hypothetical proteins and lack significant similarity to those involved in secondary metabolite biosynthesis. The difficult genetic manipulations in the recalcitrant endogenous producer *A. orientalis* Q427-8 and unstable production of QMNs hindered further investigation of the gene cluster in vivo, and heterologous expression of the entire cluster in a surrogate host was unsuccessful. Therefore, the actual borders of the cluster were not determined.

Bioinformatic Analysis of the QMN Cluster

Three PKS genes, *qmnA1*, *qmnA2*, and *qmnA3*, encode six PKS modules containing a total of six acyltransferases (ATs), six β-ketoacyl synthases (KSs), six ACPs, four ketoreductases (KRs), and four dehydratases (DHs; Figure 2B). The first loading module (M-L) contains a mutant KS^Q domain that functions as a malonyl-thioester decarboxylase (Bisang et al., 1999), and the other KS domains are all functional due to the presence of the conserved catalytic triad of C-H-H (Figure S4A). Each AT domain bears a highly conserved active site of GHSxG (Figure S4A). A substrate-binding motif specific for malonyl-CoA (MCoA) was found in M-L, M-3, and M-5, and methylmalonyl-CoA (MMCoA) specificity-conferring residues were identified in M-1, M-2, and M-4 (Reeves et al., 2001). All ACPs contain a signature motif around the invariable 4′-phosphopantetheine attachment site Ser residue (Figure S4A), and DHs contain a conserved active site with an H-D catalytic dyad (Akey et al., 2010). The KRs contain a signature NADPH-binding site as well as an active site consisting of S-Y and LDD motifs of B-type KRs to produce a hydroxyl group of R stereochemistry (Keatinge-Clay, 2007).

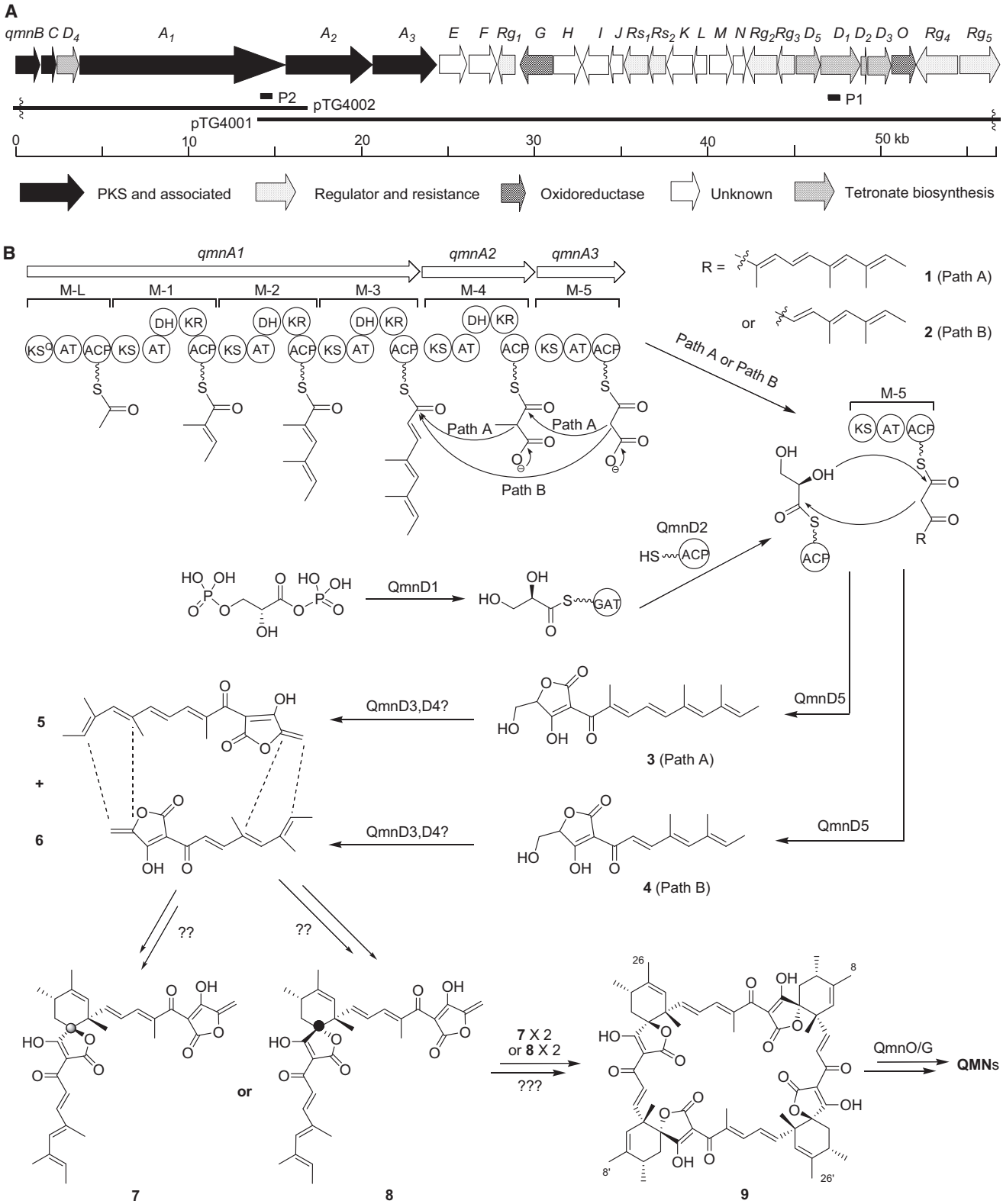

Figure 2. Biosynthetic Gene Cluster and Pathway of QMN

(A) Organization of the gene cluster.

(B) Proposed model for the biosynthesis of QMN.

See also Tables S1and S2 and Figure S4.

Table 1. Deduced Functions of ORFs in the QMN Biosynthetic Gene Cluster

Gene	Amino Acid	Protein Homolog (Accession Number[a]); Origin	Similarity/ Identity (%)	Proposed Function
Orf-3[b]	247	short-chain dehydrogenase (EHR61900.1); *Saccharomonospora cyanea* NA-134	83/77	unknown
Orf-2[b]	283	α/β hydrolase protein (ACZ87498); *Streptosporangium roseum* DSM 43021	75/64	unknown
Orf-1[b]	308	conserved hypothetical protein (EFL10610); *Streptomyces* sp. AA4	82/73	unknown
qmnB	471	AccD6 (AAS04317); *Mycobacterium avium* subsp. *paratuberculosis* K-10	77/64	propionyl-CoA carboxylase
qmnC	251	thioesterase (EFN18142); *S. violaceusniger* Tu 4113	80/65	TE II
qmnD4	322	ChlD4 (AAZ77706); *S. antibioticus*	63/50	2-oxoacid dehydrogenase/AT
qmnA1	5924	KijS1 (ACB46488); *Actinomadura kijaniata*	63/52	PKS (KS^Q-AT-ACP-KS -AT-DH-KR-ACP-KS-AT-DH-KR-ACP-KS-AT-DH-KR-ACP)
qmnA2	1771	ORF 20 (ABM47021); *A. orientalis*	66/54	PKS (KS-AT-DH-KR-ACP)
qmnA3	1292	ChlA6 (AAZ77699); *S. antibioticus*	71/60	PKS (KS-AT-ACP)
qmnE	412	β-lactamase (EFL23320); *S. himastatinicus* ATCC 53653	66/56	unkown
qmnF	396	cysteine desulfurase (EFL10316); *S.* sp. AA4	67/54	unknown
qmnRg1	255	ChlF2 (AAZ77687); *S. antibioticus*	71/59	regulator
qmnG	533	Ken10 (CAQ52613); *S. violaceoruber*	74/61	PQQ-dependent dehydrogenase
qmnH	376	–	–	unknown
qmnI	348	hypothetical protein SrosN15_20443 (ZP_04695314); *S. roseosporus* NRRL 15998	54/36	unknown
qmnJ	161	conserved hypothetical protein (ADH70169); *Nocardiopsis dassonvillei* subsp. *dassonvillei* DSM 4311	57/35	unknown
qmnRs1	392	ABC transporter-like protein (EDY52293); *S. clavuligerus* ATCC 27064	70/54	transporter
qmnRs2	227	macrolide efflux ABC transporter (EFF80341); *Actinomyces odontolyticus* F0309	78/61	transporter
qmnK	352	peptidoglycan-binding domain 1 protein (EFN14959); *S. violaceusniger* Tu 4113	54/37	unknown
qmnL	152	hypothetical protein Ndas_4785 (ADH70169); *Nocardiopsis dassonvillei* subsp. *dassonvillei* DSM 43111	51/33	unknown
qmnM	219	hypothetical protein SVEN_6245 (CCA59531); *S. venezuelae* ATCC 10712	51/41	unknown
qmnN	130	hypothetical protein SVEN_6245 (CCA59531); *S. venezuelae* ATCC 10712	53/39	unknown
qmnRg2	449	putative two-component sensor kinase (CAJ62689); *Frankia alni* ACN14a	69/60	regulator
qmnRg3	222	two-component system response regulator (CAJ62690); *Frankia alni* ACN14a	88/80	regulator
qmnD5	343	ChlM (AAZ77702); *S. antibioticus*	75/62	3-oxoacyl-ACP synthase III (KS)
qmnD1	613	ChlD1 (AAZ77703); *S. antibioticus*	73/62	glyceryltransferase/phosphatase
qmnD2	71	Tmn7a (BAF73715); *S.* sp. NRRL 11266	77/65	ACP
qmnD3	281	Tmn7 (BAE93721); *S.* sp. NRRL 11266	76/65	2-oxoacid dehydrogenase/AT
qmnO	403	FadC (AAW81703); *Pseudonocardia autotrophica*	72/56	cytochrome P450
qmnRg4	935	LuxR family transcriptional regulator (CAM02144); *Saccharopolyspora erythraea* NRRL 2338	66/52	regulator
qmnRg5	821	SARP family transcriptional regulator (ACU37101); *Actinosynnema mirum* DSM 43827	55/44	regulator
orf(+1)[b]	734	probable exodeoxyribonuclease V (AAG23283); *Saccharopolyspora spinosa*	91/84	exodeoxyribonuclease
orf(+2)[b]	240	precorrin 6A synthase (ABD12019); *Frankia* sp. CcI3	75/62	precorrin 6A synthase
orf(+3)[b]	435	NADH dehydrogenase (EFL07579.1); *Streptomyces* sp. AA4	81/74	NADH dehydrogenase

[a]Accession numbers deposited in the GenBank database.
[b]*orfs* beyond the QMN gene cluster.

These domains are all consistent with the structure of long polyketide chain **1**, which was hypothesized to be an intermediate of path A for the biosynthesis of QMN (Figure 2B). In addition, a propionyl-CoA carboxylase (QmnB) and type II thioesterase (QmnC) involved in this pathway were considered to be responsible for providing the MMCoA precursor and editing aberrant polyketide intermediates on a PKS assembly line, respectively.

As expected, the presence of homologs of the five conserved genes (*qmnD1–D5*) in the QMN cluster further supports the common unifying paradigm for tetronate biosynthesis, which is also consistent with the ABY cluster that was recently genetically characterized (Gottardi et al., 2011). These gene products show extremely high homology to the enzymes involved in CHL and TMN biosynthesis (50%–65% identity and 60%–75% similarity). Based on studies showing that RkD, an FabH-like β-ketoacyl-ACP synthase III (KS III), is required for RK-682 formation from ACP-bound substrates (Sun et al., 2010), we concluded that QmnD1, similarly to ChlD1, KijC, Tmn16, TcaD1, RkE, and AbyA2, provides both glyceryltransferase and phosphatase (GAT) activities to load a three-carbon glyceroyl group from 1,3-BPG onto QmnD2 (a discrete ACP homologous to ChlD2, KijD, Tmn7a, TcaD2, RkF, and AbyA3), yielding glyceryl-*S*-ACP. QmnD5 (homologous to ChlM, KijB, Tmn15, TcaD4, RkD, and AbyA1) may catalyze C-C and C-O bond formation from glyceryl-*S*-ACP and the ACP-*S*-tethered nascent polyketide chain to generate tetronate intermediates **3** and **4** (Figure 2B). Additional comparative analyses of QMN, TMN, ABY, and RK-682 biosynthetic machinery revealed that QmnD3 and QmnD4 (the 2-oxoacid dehydrogenase/AT homologs, similar to ChlD3/ChlD4, KijE, Tmn7/Tmn17, TcaD3, and AbyA4/AbyA5) may catalyze the dehydration of intermediates **3** and **4** to yield intermediates **5** and **6** (Figure 2B).

QmnO contains a typical heme-binding motif (FGHGAHxCLG) and is homologous to the known cytochrome P450 oxidase FadC (Chen et al., 2005). It is also a candidate enzyme for hydroxylation at C-8, C-8′, C-26, and C-26′ of QMN (Figure 1B). QmnG bears a conserved pyrrolo-quinolinequinone (PQQ)-binding motif and shows high sequence homology to Ken10 (61% identity and 74% similarity), which is a putative PQQ-dependent alcohol dehydrogenase from the kendomycin biosynthetic pathway (Wenzel et al., 2008). Therefore, it may be responsible for further oxidization of the hydroxyl group into aldehyde at the C-8 and C-8′ positions, both of which have been proposed to tailor modification steps involved in the production of QMNs from intermediate **9** (Figure 2B). In addition, QmnE exhibits sequence homology to β-lactamase (56% identity and 66% similarity), and QmnF shows similarity to pyridoxal phosphate (PLP)-dependent cysteine desulfurase (54% identity and 67% similarity). However, the exact roles of these proteins in the QMN biosynthetic pathway remain to be elucidated.

Five genes encode putative regulatory proteins, including a ChlF2-like regulator (QmnRg1), a pair of two-component regulators (QmnRg2-Rg3), a LuxR family regulator (QmnRg4), and a SARP family activator (QmnRg5). Two genes within this cluster, *qmnRs1* and *qmnRs2*, encode ABC transporters as resistant proteins to ensure efficient self-protection. In addition, there are seven genes (*qmnH*, *qmnI*, *qmnJ*, *qmnK*, *qmnL*, *qmnM*, and *qmnN*) encoding proteins that either show no obvious homology to any proteins in the databases or resemble proteins with unknown functions. Therefore, the roles of these genes in QMN biosynthesis could not be predicted by sequence analysis.

Biochemical Characterization of Long Polyketide Chain Biosynthesis through Path A by a Colinearity Model

The QMN PKS contains six modules that are consistent with the structure of long polyketide chain **1** following the colinearity model (path A in Figure 2B). To explore the biosynthesis of **1** in vitro, the M-4 protein QmnA2, which contains five domains with KS-AT-DH-KR-ACP organization, was separated, expressed, and purified as two proteins: QmnA2′ (KS4-AT4-DH4-KR4) and ACP4 from *Escherichia coli* BL21 (DE3). In addition, ACP3-1 (the ACP domain of M-3 containing N-His_6 tag), QmnA3, and ACP5 (the ACP domain of M-5) were also expressed and purified for use in the biochemical assay (Figure S5). Using 4′-phosphopantetheinyltransferase (Sfp; Quadri et al., 1998), intermediate **11-1** was synthesized with polyketide-CoA **10** and apo-ACP3 as substrates (Figure 3A). When the assay containing **11-1** was combined with QmnA2′, holo-ACP4, and MM-CoA, an elongated product **12** was observed by high-performance liquid chromatography (HPLC) and liquid chromatography-mass spectroscopy (LC-MS) analysis (Figure 3B; Figure S7; Table S3). In addition, the further modification product **13** also appeared by following NADPH-dependent ketoreduction and dehydration catalyzed by KR and DH domains (Figure 3B; Figure S7; Table S3). Next, when **13** (which was also produced by Sfp using polyketide-CoA **14** and apo-ACP4) and MCoA were incubated with QmnA3 and holo-ACP5 together, the polyketide elongation product **1** was produced, which was supported by the generation of derivative **15**, as detected by HPLC analysis and further confirmed by LC-MS (Figure 3C; Figure S8; Table S3). The concomitant decrease of substrates holo-ACP5 and **13** and increase in the products holo-ACP4 and **15** (Figure 3C) is consistent with the expected results of polyketide chain elongation.

Biochemical Characterization of Short Polyketide Chain Biosynthesis through Path B by Module Skipping

Because no additional PKS modules were identified in the presumed cluster, we hypothesized that the short polyketide chain was also constructed by the same PKS assembly line. However, in order to fit the short polyketide chain **2**, the M-4 protein QuaA2 should be programmably skipped during the PKS assembly (path B in Figure 2B). To verify this module skipping mechanism, another protein, ACP3-2, was expressed and purified (also the ACP domain of M-3 containing N-His_6 and C-His_6; the retention time in HPLC analysis was slightly different from ACP3-1). Similarly, **11-2** was synthesized using polyketide-CoA **10** and apo-ACP3-2 as substrates catalyzed by Sfp (Figure 3A). When **11-2** and M-CoA were incubated with QmnA3 and holo-ACP5 together, the polyketide elongation product **2** was produced and followed by thioester exchanging to yield **16**, which was detected by HPLC analysis and further confirmed by LC-MS (Figure 3D; Figure S9; Table S3). In addition, the change in the ratios between substrates and products also supports the expected enzymatic reactions.

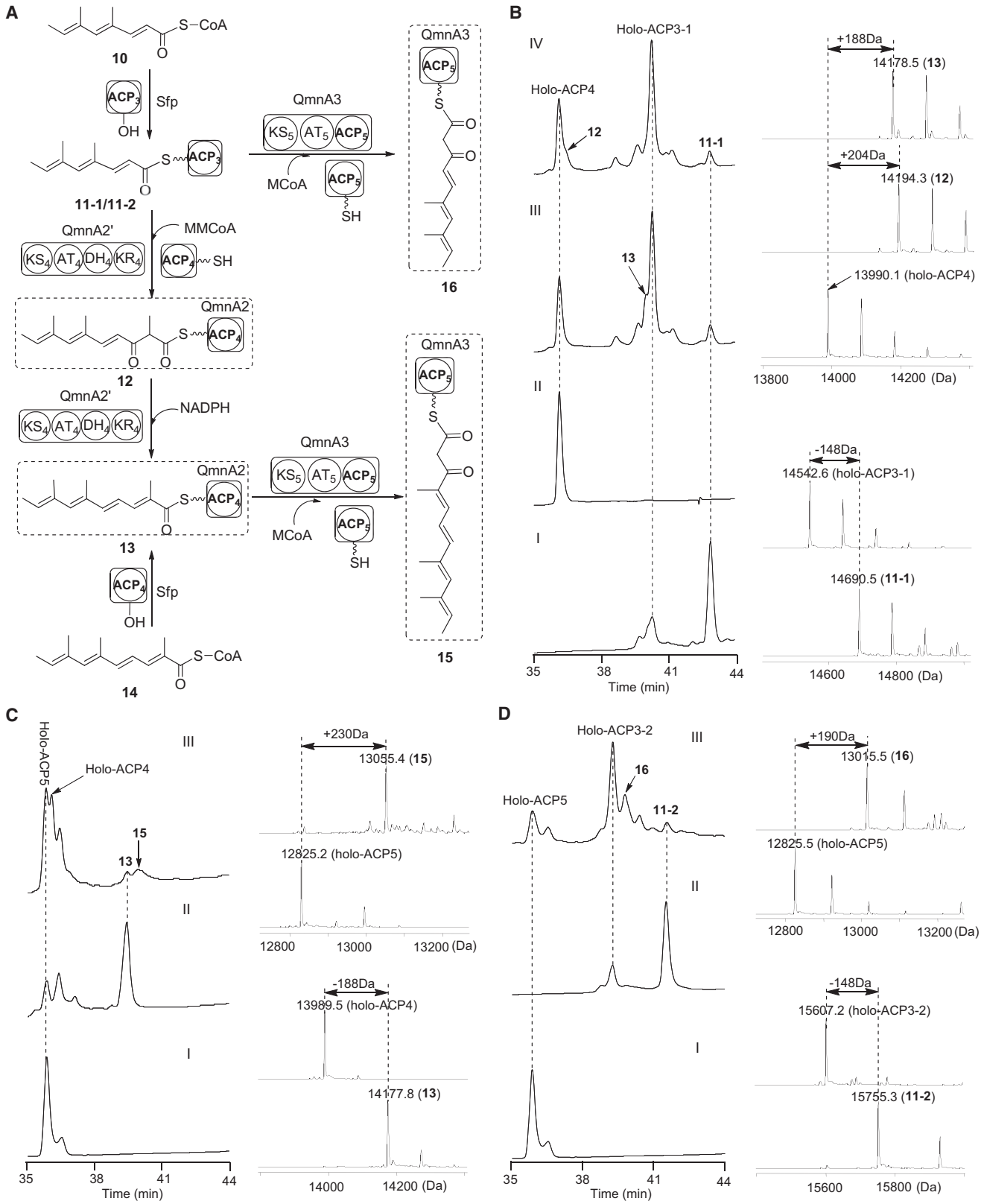

Figure 3. In Vitro Biochemical Characterization of PKS Module Skipping Involved in QMN Biosynthesis

(A) Biochemical investigations of QmnA2′ and QmnA3. The intermediates **11-1** and **11-2** were prepared by incubating **10** and Sfp with apo- ACP3-1 (N-His_6 tag) or apo-ACP3-2 (N-His_6 and C-His_6 tag), respectively.

Reconstruction of Tetronate Building-Block Biosynthesis In Vitro

To date, TcaD1 in the TCA pathway (Fang et al., 2008), Tmn16 in the TMN biosynthesis pathway (Sun et al., 2008), and RkE in the RK-682 biosynthesis pathway (Sun et al., 2010) have been biochemically confirmed to have GAT activities. However, only RkD in the RK-682 biosynthetic pathway was proposed to catalyze C-C and C-O bond formation based on in vitro data (Sun et al., 2010). Therefore, we first cloned *qmnD1*, *qmnD2*, *qmnD5*, and *qmnA3-ACP5* genes, heterologously expressed them in *E. coli* BL21 (DE3), and purified the respective proteins to homogeneity (Figure S5). HPLC and electrospray ionization (ESI)-MS analysis confirmed that QmnD2 (ACP) is in apo-form (Figure 4BI; Figure S6; Table S3). When it was incubated with CoA and the Sfp, apo-ACP was converted into the functional holo form (Figure 4BII; Figure S10). To verify glyceryl transfer reactions catalyzed by QmnD1, the purified protein was incubated with ATP, Mg^{2+}, *D*-3-phosphoglycerate (3-PG), and 3-PG kinase for generation of 1,3-BPG in situ, and then the holo-QmnD2 was added to directly test glyceryl loading (Figure 4A). Reaction mixtures were subjected to HPLC analysis (Figure 4BIII) and the reaction products were also subjected to quadrupole time-of-flight (Q-TOF)-MS analysis. As expected, the addition of 88.0 Da to holo-QmnD2 to generate **17** was in exact agreement with the mass increase for glycerate (Figure 4C; Figure S4; Table S3). We then synthesized **16** using the polyketide-CoA **18** and apo-ACP5 as substrates catalyzed by Sfp (Figure 4BIV; Figure S10). When **16** and **17** were incubated with QmnD5 together, HPLC analysis confirmed that the decrease of substrates was obvious (Figure 4BV) and the tetronate product **4** was detected by analysis of the reaction products using LC-MS (Figure 4D). This was further confirmed by MS/MS (Figure 4E). Together, these in vitro results strongly support the notion that 1,3-BPG can be effectively activated by QmnD1 and subsequently dephosphorylated. This step is followed by the transfer onto holo-QmnD2 to form glyceryl-*S*-ACP intermediate **17**, and subsequent coupling with the QmnA3-ACP5-tethered nascent polyketide chain catalyzed by QmnD5 to produce tetronate intermediate **4** (Figure 4A).

DISCUSSION

In most cases, modular PKSs synthesize polyketides through successive Claisen condensations, and one module is responsible for one round of chain extension. However, an increasing number of exceptions are being characterized, revealing other strategies beyond the colinearity model for an assembly line of modular PKS (Moss et al., 2004). One well-described example is pikromycin PKS, which generates 12- and 14-membered ring macrolactones, most likely through a programmed module skipping mechanism (Xue and Sherman, 2000; Beck et al., 2002, 2003; Aldrich et al., 2005). Another PKS module skipping phenomenon was observed in an engineered PKS system in which both triketides and tetraketides were identified, and an ACP transfer step was required to facilitate transfer of the substrate over long distances (Thomas et al., 2002). In addition, for nonribosomal peptide synthetase systems, myxochromide S in *Stigmatella aurantiaca* was biosynthesized using a module skipping process induced by a natural point mutation (Wenzel et al., 2006). In the QMN biosynthetic pathway, we hypothesized and biochemically confirmed that the QmnA1-QmnA2-QmnA3 PKS not only catalyzed the synthesis of long polyketide chain **1** (path A in Figure 2B) but also produced short polyketide chain **2** (path B in Figure 2B). These findings suggested that the C-terminal docking domain of QmnA1 could recognize not only the N-terminal docking domain of QmnA2 but also the N-terminal docking domain of QmnA3, whereas the C-terminal docking domain of QmnA2 could only interact with the N-terminal docking domain of QmnA3. According to structural information about docking domains in PKS genes (Broadhurst et al., 2003; Buchholz et al., 2009), all of the docking domains bear conserved residues and contain well-matched amino acids for possible salt bridges (Figure S4B). Two distinct mechanisms can be considered for QMN polyketide chains biosynthesis: In one mechanism, the QmnA1-QmnA2-QmnA3 assembly line may be arranged by a linear mode, and the short polyketide chain **2** may be produced through a complete-module skipping mechanism, similarly to the biosynthesis of myxochromide S. In the other mechanism, QmnA1-QmnA2-QmnA3 may also be clustered, in which case both domain KS4 and domain KS5 interact with domain ACP3. In addition to domain ACP3, domain KS5 also interacts with domain ACP4 simultaneously (Figure S4C).

The bioconstruction of symmetric molecules by oligomerization of the basic units through an ester or amide bond is usually mediated by the thioesterase domain, which catalyzes the cycloologomerization process (Kohli and Walsh, 2003; Watanabe et al., 2006; Cheng, 2006). QMNs bear a 32-member carbocyclic architecture consisting of four spirotetronic acid units connected by enone linkers in a head-to-tail fashion, so the carbon frameworks are composed of only C-C linkages. Two hypotheses have been proposed for the biosynthesis of QMNs: (1) stereodivergent Prins-type cyclizations for the formation of the stereoisomeric spirocylic units (Roush and Barda, 2002), or (2) stereodivergent intermolecular Diels-Alder reactions between pairs of 3-trienoyl- and 3-tetraenoyl-5-methylenefuran-2, 4-diones to form the spirotetronate and the 32-member carbocycle (Montgomery and Challis, 2008). However, to date, no genetic or biochemical information has been obtained to support these models. The biochemical investigation of QMN biosynthesis reveled that QmnD5, which is a FabH-like

(B) HPLC and Q-TOF-MS analysis of the first step of **1** biosynthesis via path A: (I) production of **11-1** using **10** and apo-ACP3-1 catalyzed by Sfp; and (II) holo-ACP4, chain elongation yielding **13** (III, in the presence of NADPH) and **12** (IV, in the absence of NADPH) catalyzed by QmnA2 using **11-1** as substrate.

(C) HPLC and Q-TOF-MS analysis of the second step of **1** biosynthesis via path A: (I) holo-ACP5, (II) production of **13** using **14** and apo-ACP4 catalyzed by Sfp, and (III) chain elongation yielding **15** catalyzed by QmnA3 using **13** as substrate.

(D) HPLC and Q-TOF-MS analysis of **2** biosynthesis via path B: (I) holo-ACP5, (II) production of **11-2** using **10** and apo-ACP3-2 catalyzed by Sfp, and (III) chain elongation yielding **16** catalyzed by QmnA3 using **10-2** as substrate.

See also Table S3 and Figures S1, S2, S4–S9, and S11–S14.

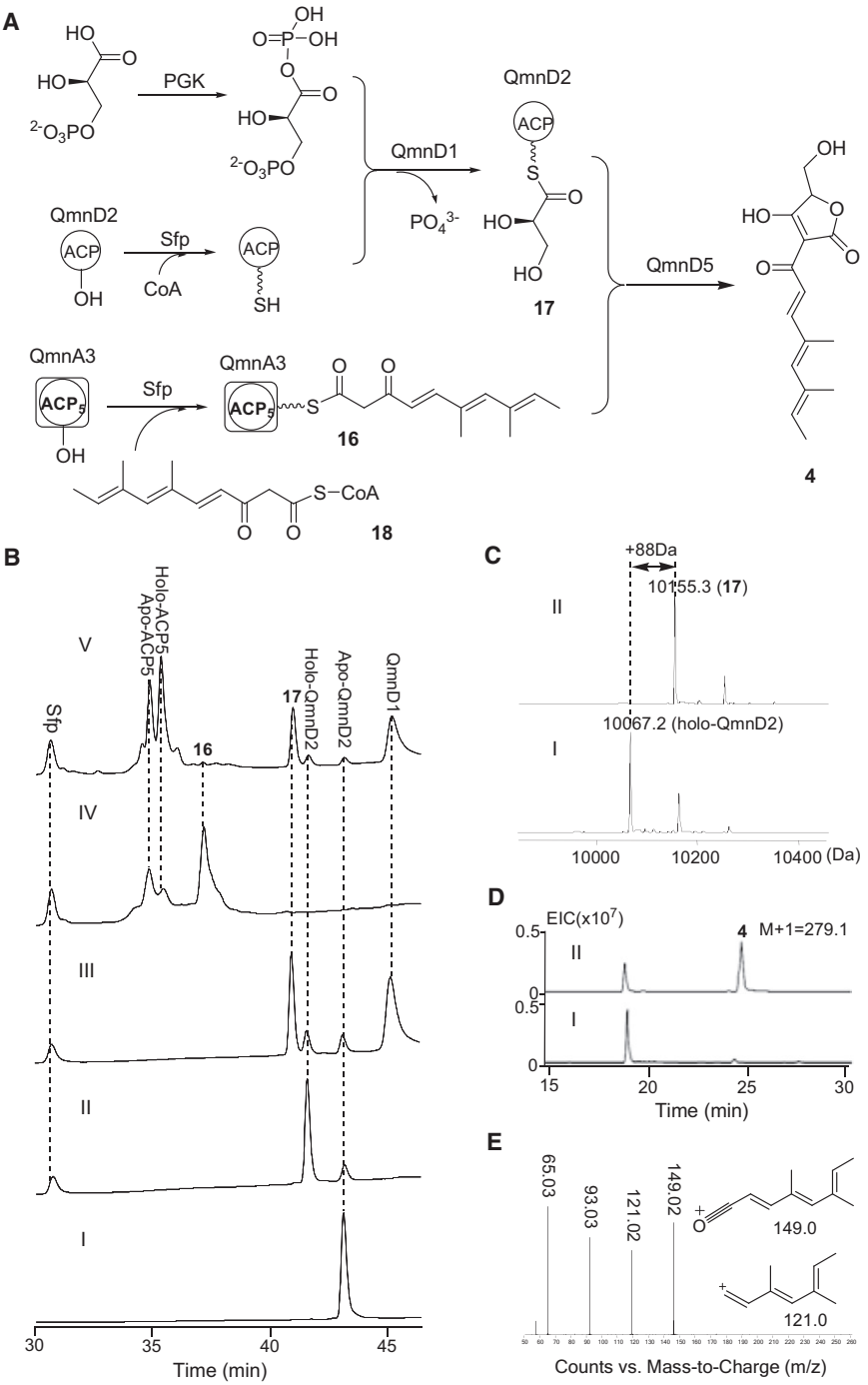

Figure 4. In Vitro Biochemical Characterization of Tetronate Biosynthesis

(A) Biochemical investigations to construct the tetronate moiety.

(B) Protein detection by HPLC analysis of purified apo-QmnD2 (I), holo-QmnD2 (II), incubated with QmnD1 (III), apo-QmnA3-ACP5 modified by Sfp in the presence of **18** (IV), and entire reaction catalyzed by QmnD5 (V).

(C) Q-TOF-MS analysis of holo-QmnD2 (I) and the generation of glyceryl-S-QmnD2 **17** (II).

(D) Chemical detection of **4** in the reaction catalyzed by QmnD5 (II) and control with denatured QmnD5 (I) by LC-MS analysis.

(E) Further confirmation of tetronate **4** production by MS/MS analysis.

See also Table S3 and Figures S3, S5, S6, S10, S15, and S16.

3-oxoacyl-ACP synthase III (KS III), catalyzes the short polyketide chain release and further tetronate intermediate **4** formation. We also suggest that the long tetronate intermediate **3** is synthesized by the only KS III, QmnD5, using the same pathway (Figure 2B). Then, QmnD3 and QmnD4 (the two-component 2-oxoacid dehydrogenase/AT-like enzymes) may catalyze the two tetronate intermediates to dehydrate and give rise to the 3-polyenoyl-5-methylenefuran-2,4-dione intermediates **5** and **6** (Figure 2B). Next, two steps of [4 + 2] cycloaddition, possibly through *exo* and *endo* Diels-Alder reactions, should be involved in the construction of symmetricaglycone **7** or **8** into **9**, which can be further modified by hydroxylation (QmnO), oxidization (QmnG), and even glycosylation to produce all members of the QMNs (Figure 2B). Therefore, the stereodivergent intermolecular Diels-Alder reaction to form the spirotetronate and the 32-member carbocycle (Montgomery and Challis, 2008) is preferred.

Although the enzyme-catalyzed [4 + 2] cycloaddition has attracted substantial attention from scientists for a long time (Oikawa and Tokiwano, 2004; Kelly, 2008), almost all of the proposed Diels-Alder cycloadditions are intramolecular cyclizations, including the lovastatin nonaketide synthase (Auclair et al., 2000), the recently characterized elansolid biosynthesis (Dehn et al., 2011), solanapyrone synthase (Kasahara et al., 2010), and the likely Diels-Alderase SpnF in the biosynthesis of spinosyn A (Kim et al., 2011; Townsend, 2011). The macrophomate synthase (MPS) is the most extensively studied of all the putative Diels-Alderases and catalyzes a total of four steps, including the intermolecular [4 + 2] cycloaddition (Ose et al., 2003). However, mixed quantum and molecular-mechanics simulations of MPS support a stepwise Michael-Aldol reaction mechanism rather than a Diels-Alder reaction (Guimarães et al., 2005). MPS was also shown to be an efficient aldolase with a series of aldehyde substrates (Serafimov et al., 2008). Therefore, our characterization of the QMN biosynthetic gene cluster in this study not only provides another opportunity to explore possible Diels-Alderases but also sets the stage for further investigations of the enzymatic process and mechanism of stereodivergent intermolecular [4 + 2] cycloaddition.

SIGNIFICANCE

QMNs belong to the group of spirotetronate natural products and have a unique symmetrical structure with four spirotetronate units. In this study, we cloned the biosynthetic gene cluster of QMNs by degenerate primer PCR amplification of specific genes involved in the biosynthesis of the tetronate moiety. Our biochemical characterization of the biosynthetic pathway suggests that there is a module skipping strategy in the process of chain extension for building the short polyketide chain, and that the module PKS assembly line can be used to synthesize two alternative polyketide chains, both of which are essential for the biosynthesis of QMNs. This is an example of bacteria adopting an economical approach for the biosynthesis of natural products. In addition, our biochemical results confirmed that 1,3-BPG was incorporated into the tetronate ring, and even showed that the tetronate moiety of spirotetronate antibiotics could be reconstructed in vitro as Rk-682. Successful construction of the tetronate moiety provides an opportunity to explore the enzymatic process and mechanism of a possible stereodivergent intermolecular [4 + 2] cycloaddition.

EXPERIMENTAL PROCEDURES

General

A QMNs producer, *A. orientalis* Q427-8 (ATCC 53884), was purchased from the American Type Culture Collection and cultured as described previously (Tsunakawa et al., 1992). *E. coli* DH5α competent cells were used for routine subcloning and plasmid preparations, and *E. coli* BL21(DE3) was used as the protein expression host. *E. coli* cells were grown in LB medium with appropriate antibiotics, when necessary. Other plasmids are summarized in Table S1. All other common biochemicals and chemicals were obtained from standard commercial sources. PCR amplification was carried out using either *Taq* DNA polymerase or PfuUltra DNA polymerase with genomic DNA or fosmid as a template, and degenerate or specific primers listed in Table S2. Primer synthesis was performed at the Invitrogen Shanghai Center. DNA sequencing was performed at Shanghai GeneCore Biotechnology Inc. Analytical HPLC was carried out on an Agilent 1200 HPLC system with a PDA detector. LC-MS analysis was carried out on an Agilent 1200 HPLC instrument connected to LCQ Fleet ESI mass spectrometer (Thermo Fisher Scientific). ESI-MS was performed with a Shimadzu LCMS-2010 EV mass spectrometer.

Genomic Library Construction, Screening, and Sequence Analysis

A genomic library of *A. orientalis* Q427-8 was constructed in the fosmid vector pCC1FOS-1 (Epicenter Technologies) according to the manufacturer's protocol. The D1 gene probes (P1) for library screening were obtained by PCR amplification with primers ChlD1-For-1 (or ChlD1-For-2) and ChlD1-Rev (Table S2), and confirmed by sequencing. The genomic library (4.0×10^3 clones) was screened by colony hybridization, and the resultant positive clones were further confirmed by PCR amplification and southern blotting. To extend the cloned DNA region on the chromosome, the library was further screened by colony hybridization with probe P2 (a 0.83-kb PCR fragment with Q-walk-For and Q-walk-Rev as primers) from pTG4001 (Figure 2A; PCR primers are summarized in Table S2). The ORFs were deduced from the sequence by means of the FramePlot 4.0beta program (http://nocardia.nih.go.jp/fp4) and BLAST methods. Amino acid sequence alignments were obtained using the CLUSTALW method with Biology WorkBench 3.2 software (http://workbench.sdsc.edu). The functional domains of the PKSs were identified by using a program available from http://www.nii.res.in/searchall.html.

Protein Expression and Purification

The DNA fragments encoding individual target proteins were amplified by PCR, using the cosmid pTG4001 as the template. The primers for the amplification are listed in Table S2. The identity of each PCR product was confirmed by sequencing. Each fragment was doubly digested with the corresponding restriction endonuclease and ligated with pET28a, pET37b, or pF7 to provide the plasmids for protein expression. The fragments coding QmnD1, QmnA1-ACP3-1, and QmnA3-ACP5 were digested by *Nde*I/HindIII and ligated with pET28a. The fragment coding QmnD2 was digested by *Nde*I/HindIII and ligated with pET37b. Both of the fragments coding QmnA1-ACP3-2 and QmnA2-ACP4 were digested by *Nde*I/*Xho*I; however, the former was ligated with pET28a and the latter was ligated with pET37b. The fragment coding QmnD5 was digested by EcoRI/HindIII and ligated with pF7. The longer genes coding QmnA2 and QmnA3 were divided into two fragments. The two fragments for QmnA2 were digested by *Nde*I/*Not*I and *Not*I/HindIII, respectively, and three-segment-ligated with pET28a. The fragments for QmnA3 were digested by *Nde*I/*Xho*I and *Xho*I/HindIII, and also three-segment-ligated with pET28a.

For overproduction of proteins, cells harboring the desired plasmid were grown in LB medium supplemented with 50 μg/ml of kanamycin. Cultures (1 l) were grown to an OD_{600} of 0.5 at 37°C and then cooled to 16°C for 30 min, and protein expression was induced by the addition of 50 μM isopropyl β-D-thiogalactopyranoside. Cultures were grown for an additional 24 hr. Purification of the His-tagged fusion protein with Ni-NTA affinity resin was performed according to the manufacturer's manual (QIAGEN), and the resultant proteins were dialyzed against 50 mM MOPS (pH 7.5), 50 mM NaCl, and 10% glycerol, and stored at −80°C.

Chemical Synthesis of Acyl-SCoA 10, 14, and 18

The reactions were monitored by thin-layer chromatography with silica gel-coated plates. Flash-column chromatography was carried out using 300–400 mesh silica gel at increased pressure. ^1H and ^{13}C NMR spectra were recorded on a Bruker Ultrashield 400 (400 MHz) spectrometer in $CDCl_3$ with tetramethylsilane as an internal standard. Chemical shifts are referenced to residual protonated solvent (δH = 7.26 and δC = 77.16 for $CDCl_3$) and given in parts per million (ppm). For ^1H NMR spectra, the multiplicity of a signal is designated by one of the following abbreviations: s, singlet; d, doublet; t, triplet; q, quartet; m, multiplet. All coupling constants, *J*, are reported in Hertz and given to the nearest 0.1 Hz. Mass spectra were recorded using ESI. Acyl-SCoA thioesters were purified by HPLC on a LC-20A3 vp HPLC system (Shimadzu) with a Venusil XBP-C18 column (AGT, 10.0 × 250 mm, 5 μm) with the following gradients at room temperature: 0–5 min, constant 95% A/5% B; 5–20 min, a linear gradient to 30% A/70% B; 20–22 min, a linear gradient to 5% A/95% B; 22–24 min, constant 5% A/95% B; 24–26 min, a linear gradient to 95% A/5% B, and 26–30 min, constant 80% A/20% B (buffer A, 10 mM NH_4OAc in H_2O; and buffer B, CH_3CN). This was performed at a flow rate of 3 ml/min with UV detection at 310 nm. The synthetic routes and details are summarized in Figures S1–S3.

In Vitro Reconstruction of Tetronate Building-Block Biosynthesis

To prepare holo-QmnD2, an assay (50 μl) containing 50 mM MOPS (pH 7.5), 10 mM $MgCl_2$, 1 mM TCEP, 5 μM Sfp, 0.25 mM CoA, and 50 μM apo-QmnD2 was incubated for 1 hr at 30°C . To prepare 1,3-BPG in situ, a reaction (30 μl) containing 50 mM MOPS (pH 7.5), 1 mM TCEP, 5 mM ATP, 0.25 mM 3-PG, 2 U 3-PG kinase, and 5 μM QmnD1 was incubated for 30 min at 30°C. A portion of the reaction (20 μl) mixture was then added to the reaction (30 μl) containing holo-ACP as described above and incubated at 30°C for 30 min. To prepare **16**, an assay (50 μl) containing 50 mM MOPS (pH 7.5), 10 mM $MgCl_2$, 1 mM TCEP, 5 μM Sfp, 0.25 mM CoA 18, and 50 μM Qmn-ACP5 was incubated for 1 hr at 30°C, and then the portion containing glyceroyl-S-ACP5 (50 μM; as described above) and 10 μM QmnD5 was added for 6 hr. The reaction mixture was acidified with 1N HCl to pH 3, extracted with ethyl acetate, and evaporated. The residue was dissolved in MeOH and analyzed by LC-MS.

Biochemical Characterization of Polyketide Chain Biosynthesis

To prepare holo-ACP4 (or holo-ACP5), an assay (100 μl) containing 50 mM MOPS (pH 7.5), 10 mM $MgCl_2$, 1 mM TCEP, 5 μM Sfp, 0.25 mM CoA, and 50 μM apo-ACP4 (or apo-ACP5) was incubated for 1 hr at 30°C.

An assay (50 μl) containing 50 mM MOPS (pH 7.5), 10 mM $MgCl_2$, 1 mM TCEP, 5 μM Sfp, 0.25 mM **10** (or **14**), and 50 μM apo-ACP3-2 (or apo-ACP4,

apo-ACP3-1) was incubated to prepare **11-2** (or **13**, **11-1**) at 30°C for 1 hr, and then QmnA2 (or QmnA3; 5 μM) was added. After incubation at 30°C for 1 hr, MM-CoA (or M-CoA; 0.25 mM), NADPH (1 mM) and 50 μl holo- ACP4 (or holo-ACP5; 50 μM) were added. One assay in the absence of NADPH was the control reaction.

Protein assays were analyzed by HPLC with a GraceVydac protein and peptide C18 column with the following gradients at room temperature: 0–3 min, constant 80% A/20% B; 3–30 min, a linear gradient to 60% A/40% B; 30–50 min, a linear gradient to 40% A/60% B; 50–52 min, a linear gradient to 5% A/95% B; 52–54 min, constant 5% A/95% B; 54–56 min, a linear gradient to 80% A/20% B, and 26–30 min, constant 80% A/20% B (buffer A, 0.1% TFA in H_2O; buffer B, 0.1% TFA in CH_3CN). This was performed at a flow rate of 1 ml/min with UV detection at 220 nm. MS analysis was carried out with an Agilent 6530 Accurate-Mass Q-TOF LC/MS. Analysis of small molecules was carried out with a Venusil XBP-C18 column with the following gradients: 0–5 min, constant 95A/20% B; 5–25 min, a linear gradient to 5% A/95% B; and 25–40 min, a linear gradient to 5% A/95% B (buffer A, 0.1% HCOOH and 10 mM NH_4OAc in H_2O; and buffer B, 0.1% HCOOH in CH_3CN).

ACCESSION NUMBERS

The sequence reported in this paper has been deposited in GenBank under accession no. JF970188.

SUPPLEMENTAL INFORMATION

Supplemental Information includes 16 figures and three tables and can be found with this article online at http://dx.doi.org/10.1016/j.chembiol.2012.07.024.

ACKNOWLEDGMENTS

We thank the members of Prof. Zixin Deng's laboratory (Shanghai Jiao Tong University) for support in obtaining MS data of proteins. This work was supported in part by grants from National Basic Research Program of China (973 Program; Grants 2010CB833200 and 2009CB118901), the National Natural Science Foundation of China (21072214, 90913005, 20832009, and 20921091), and the Chinese Academy of Sciences.

Received: May 7, 2012
Revised: July 10, 2012
Accepted: July 30, 2012
Published: October 25, 2012

REFERENCES

Akey, D.L., Razelun, J.R., Tehranisa, J., Sherman, D.H., Gerwick, W.H., and Smith, J.L. (2010). Crystal structures of dehydratase domains from the curacin polyketide biosynthetic pathway. Structure *18*, 94–105.

Aldrich, C.C., Beck, B.J., Fecik, R.A., and Sherman, D.H. (2005). Biochemical investigation of pikromycin biosynthesis employing native penta- and hexaketide chain elongation intermediates. J. Am. Chem. Soc. *127*, 8441–8452.

Ashton, R.J., Kenig, M.D., Luk, K., Planterose, D.N., and Scott-Wood, G. (1990). MM 46115, a new antiviral antibiotic from *Actinomadura pelletieri*. Characteristics of the producing cultures, fermentation, isolation, physicochemical and biological properties. J. Antibiot. *43*, 1387–1393.

Auclair, K., Sutherland, A., Kennedy, J., Witter, D.J., Van den Heever, J.P., Hutchinson, C.R., and Vederas, J.C. (2000). Lovastatin nonaketide synthase catalyzes an intramolecular Diels-Alder reaction of a substrate analogue. J. Am. Chem. Soc. *122*, 11519–11520.

Beck, B.J., Yoon, Y.J., Reynolds, K.A., and Sherman, D.H. (2002). The hidden steps of domain skipping: macrolactone ring size determination in the pikromycin modular polyketide synthase. Chem. Biol. *9*, 575–583.

Beck, B.J., Aldrich, C.C., Fecik, R.A., Reynolds, K.A., and Sherman, D.H. (2003). Substrate recognition and channeling of monomodules from the pikromycin polyketide synthase. J. Am. Chem. Soc. *125*, 12551–12557.

Bisang, C., Long, P.F., Cortés, J., Westcott, J., Crosby, J., Matharu, A.L., Cox, R.J., Simpson, T.J., Staunton, J., and Leadlay, P.F. (1999). A chain initiation factor common to both modular and aromatic polyketide synthases. Nature *401*, 502–505.

Broadhurst, R.W., Nietlispach, D., Wheatcroft, M.P., Leadlay, P.F., and Weissman, K.J. (2003). The structure of docking domains in modular polyketide synthases. Chem. Biol. *10*, 723–731.

Buchholz, T.J., Geders, T.W., Bartley, F.E., 3rd, Reynolds, K.A., Smith, J.L., and Sherman, D.H. (2009). Structural basis for binding specificity between subclasses of modular polyketide synthase docking domains. ACS Chem. Biol. *4*, 41–52.

Chen, C.-H., Cheng, J.-C., Cho, Y.-C., and Hsu, W.-H. (2005). A gene cluster for the fatty acid catabolism from *Pseudonocardia autotrophica* BCRC12444. Biochem. Biophys. Res. Commun. *329*, 863–868.

Cheng, Y.-Q. (2006). Deciphering the biosynthetic codes for the potent anti-SARS-CoV cyclodepsipeptide valinomycin in *Streptomyces tsusimaensis* ATCC 15141. ChemBioChem *7*, 471–477.

Dehn, R., Katsuyama, Y., Weber, A., Gerth, K., Jansen, R., Steinmetz, H., Höfle, G., Müller, R., and Kirschning, A. (2011). Molecular basis of elansolid biosynthesis: evidence for an unprecedented quinone methide initiated intramolecular Diels-Alder cycloaddition/macrolactonization. Angew. Chem. Int. Ed. Engl. *50*, 3882–3887.

Demydchuk, Y., Sun, Y., Hong, H., Staunton, J., Spencer, J.B., and Leadlay, P.F. (2008). Analysis of the tetronomycin gene cluster: insights into the biosynthesis of a polyether tetronate antibiotic. ChemBioChem *9*, 1136–1145.

Fang, J., Zhang, Y., Huang, L., Jia, X., Zhang, Q., Zhang, X., Tang, G.-L., and Liu, W. (2008). Cloning and characterization of the tetrocarcin A gene cluster from *Micromonospora chalcea* NRRL 11289 reveals a highly conserved strategy for tetronate biosynthesis in spirotetronate antibiotics. J. Bacteriol. *190*, 6014–6025.

Gottardi, E.M., Krawczyk, J.M., von Suchodoletz, H., Schadt, S., Mühlenweg, A., Uguru, G.C., Pelzer, S., Fiedler, H.P., Bibb, M.J., Stach, J.E., and Süssmuth, R.D. (2011). Abyssomicin biosynthesis: formation of an unusual polyketide, antibiotic-feeding studies and genetic analysis. ChemBioChem *12*, 1401–1410.

Guimarães, C.R.W., Udier-Blagović, M., and Jorgensen, W.L. (2005). Macrophomate synthase: QM/MM simulations address the Diels-Alder versus Michael-Aldol reaction mechanism. J. Am. Chem. Soc. *127*, 3577–3588.

Jia, X.-Y., Tian, Z.-H., Shao, L., Qu, X.-D., Zhao, Q.-F., Tang, J., Tang, G.-L., and Liu, W. (2006). Genetic characterization of the chlorothricin gene cluster as a model for spirotetronate antibiotic biosynthesis. Chem. Biol. *13*, 575–585.

Kawashima, A., Nakamura, Y., Ohta, Y., Akama, T., Yamagishi, M., and Hanada, K. (1992). New cholesterol biosynthesis inhibitors MC-031 (O-demethylchlorothricin), -032 (O-demethylhydroxychlorothricin), -033 and -034. J. Antibiot. *45*, 207–212.

Kasahara, K., Miyamoto, T., Fujimoto, T., Oguri, H., Tokiwano, T., Oikawa, H., Ebizuka, Y., and Fujii, I. (2010). Solanapyrone synthase, a possible Diels-Alderase and iterative type I polyketide synthase encoded in a biosynthetic gene cluster from *Alternaria solani*. ChemBioChem *11*, 1245–1252.

Keatinge-Clay, A.T. (2007). A tylosin ketoreductase reveals how chirality is determined in polyketides. Chem. Biol. *14*, 898–908.

Kelly, W.L. (2008). Intramolecular cyclizations of polyketide biosynthesis: mining for a "Diels-Alderase"? Org. Biomol. Chem. *6*, 4483–4493.

Kim, H.J., Ruszczycky, M.W., Choi, S.H., Liu, Y.-N., and Liu, H.-W. (2011). Enzyme-catalysed [4+2] cycloaddition is a key step in the biosynthesis of spinosyn A. Nature *473*, 109–112.

Kohli, R.M., and Walsh, C.T. (2003). Enzymology of acyl chain macrocyclization in natural product biosynthesis. Chem. Commun. (Camb.) *3*, 297–307.

Kusumi, T., Ichikawa, A., Kakisawa, H., Tsunakawa, M., Konishi, M., and Oki, T. (1991). The structures of quartromicins A1, A2, and A3: novel macrocyclic antiviral antibiotics possessing four tetronic acid moieties. J. Am. Chem. Soc. *113*, 8947–8948.

Montgomery, L.J., and Challis, G.L. (2008). Concise synthesis of key 3-polyenoyl-5-methylenefuran-2,4-dione putative intermediates in quartromicin biosynthesis. Synlett, 2164–2168.

Moss, S.J., Martin, C.J., and Wilkinson, B. (2004). Loss of co-linearity by modular polyketide synthases: a mechanism for the evolution of chemical diversity. Nat. Prod. Rep. *21*, 575–593.

Ohtsuka, T., Kotaki, H., Nakayama, N., Itezono, Y., Shimma, N., Kudoh, T., Kuwahara, T., Arisawa, M., Yokose, K., and Seto, H. (1993). Tetronothiodin, a novel cholecystokinin type-B receptor antagonist produced by *Streptomyces* sp. NR0489. II. Isolation, characterization and biological activities. J. Antibiot. *46*, 11–17.

Oikawa, H., and Tokiwano, T. (2004). Enzymatic catalysis of the Diels-Alder reaction in the biosynthesis of natural products. Nat. Prod. Rep. *21*, 321–352.

Ose, T., Watanabe, K., Mie, T., Honma, M., Watanabe, H., Yao, M., Oikawa, H., and Tanaka, I. (2003). Insight into a natural Diels-Alder reaction from the structure of macrophomate synthase. Nature *422*, 185–189.

Quadri, L.E., Weinreb, P.H., Lei, M., Nakano, M.M., Zuber, P., and Walsh, C.T. (1998). Characterization of Sfp, a *Bacillus subtilis* phosphopantetheinyl transferase for peptidyl carrier protein domains in peptide synthetases. Biochemistry *37*, 1585–1595.

Reeves, C.D., Murli, S., Ashley, G.W., Piagentini, M., Hutchinson, C.R., and McDaniel, R. (2001). Alteration of the substrate specificity of a modular polyketide synthase acyltransferase domain through site-specific mutations. Biochemistry *40*, 15464–15470.

Riedlinger, J., Reicke, A., Zähner, H., Krismer, B., Bull, A.T., Maldonado, L.A., Ward, A.C., Goodfellow, M., Bister, B., Bischoff, D., et al. (2004). Abyssomicins, inhibitors of the para-aminobenzoic acid pathway produced by the marine *Verrucosispora* strain AB-18-032. J. Antibiot. *57*, 271–279.

Roush, W.R., and Barda, D.A. (2002). Partial stereochemical assignment of quartromicins A_3 and D_3. Org. Lett. *4*, 1539–1542.

Serafimov, J.M., Gillingham, D., Kuster, S., and Hilvert, D. (2008). The putative Diels-Alderase macrophomate synthase is an efficient aldolase. J. Am. Chem. Soc. *130*, 7798–7799.

Sun, Y., Hong, H., Gillies, F., Spencer, J.B., and Leadlay, P.F. (2008). Glyceryl-S-acyl carrier protein as an intermediate in the biosynthesis of tetronate antibiotics. ChemBioChem *9*, 150–156.

Sun, Y., Hahn, F., Demydchuk, Y., Chettle, J., Tosin, M., Osada, H., and Leadlay, P.F. (2010). *In vitro* reconstruction of tetronate RK-682 biosynthesis. Nat. Chem. Biol. *6*, 99–101.

Tanabe-Tochikura, A., Nakashima, H., Murakami, T., Tenmyo, O., Oki, T., and Yamamoto, N. (1992). Anti-human immunodeficiency virus (HIV) activity of the novel antiviral antibiotic quartromicins which enhance inhibitory effect of 3′-azido-2′,3′-dideoxythymidine (AZT) in vitro. Antivir. Chem. Chemother. *3*, 345–349.

Thomas, I., Martin, C.J., Wilkinson, C.J., Staunton, J., and Leadlay, P.F. (2002). Skipping in a hybrid polyketide synthase. Evidence for ACP-to-ACP chain transfer. Chem. Biol. *9*, 781–787.

Tomita, F., Tamaoki, T., Shirahata, K., Kasai, M., Morimoto, M., Ohkubo, S., Mineura, K., and Ishii, S. (1980). Novel antitumor antibiotics, tetrocarcins. J. Antibiot. *33*, 668–670.

Townsend, C.A. (2011). A "Diels-Alderase" at last. ChemBioChem *12*, 2267–2269.

Tsunakawa, M., Tenmyo, O., Tomita, K., Naruse, N., Kotake, C., Miyaki, T., Konishi, M., and Oki, T. (1992). Quartromicin, a complex of novel antiviral antibiotics. I. Production, isolation, physico-chemical properties and antiviral activity. J. Antibiot. *45*, 180–188.

Waitz, J.A., Horan, A.C., Kalyanpur, M., Lee, B.K., Loebenberg, D., Marquez, J.A., Miller, G., and Patel, M.G. (1981). Kijanimicin (Sch 25663), a novel antibiotic produced by *Actinomadura kijaniata* SCC 1256. Fermentation, isolation, characterization and biological properties. J. Antibiot. *34*, 1101–1106.

Watanabe, K., Hotta, K., Praseuth, A.P., Koketsu, K., Migita, A., Boddy, C.N., Wang, C.C., Oguri, H., and Oikawa, H. (2006). Total biosynthesis of antitumor nonribosomal peptides in *Escherichia coli*. Nat. Chem. Biol. *2*, 423–428.

Wenzel, S.C., Meiser, P., Binz, T.M., Mahmud, T., and Müller, R. (2006). Nonribosomal peptide biosynthesis: point mutations and module skipping lead to chemical diversity. Angew. Chem. Int. Ed. Engl. *45*, 2296–2301.

Wenzel, S.C., Bode, H.B., Kochems, I., and Müller, R. (2008). A type I/type III polyketide synthase hybrid biosynthetic pathway for the structurally unique ansa compound kendomycin. ChemBioChem *9*, 2711–2721.

Xue, Y., and Sherman, D.H. (2000). Alternative modular polyketide synthase expression controls macrolactone structure. Nature *403*, 571–575.

Zhang, H., White-Phillip, J.A., Melançon, C.E., 3rd, Kwon, H.-J., Yu, W.L., and Liu, H.-W. (2007). Elucidation of the kijanimicin gene cluster: insights into the biosynthesis of spirotetronate antibiotics and nitrosugars. J. Am. Chem. Soc. *129*, 14670–14683.

Zhao, W., Zhong, Y., Yuan, H., Wang, J., Zheng, H., Wang, Y., Cen, X., Xu, F., Bai, J., Han, X., et al. (2010). Complete genome sequence of the rifamycin SV-producing *Amycolatopsis mediterranei* U32 revealed its genetic characteristics in phylogeny and metabolism. Cell Res. *20*, 1096–1108.